processes

MDPI

Article

Pyrolysis and Volatile Evolution Behaviors of Cold-Rolling Oily Sludge

Zhigang Que [1,*], Yinxuan Fu [1], Jinming Shi [1], Xianbin Ai [1] and Chunbao Xu [2,*]

[1] Institute of Energy Research, Jiangxi Academy of Science, Nanchang 330096, China; fuyinxuan_2007@163.com (Y.F.); shijinming0012@163.com (J.S.); axbustb@sina.com (X.A.)
[2] Department of Chemical and Biochemical Engineering, Western University, London, ON N6A 5B9, Canada
* Correspondence: quezhigang@126.com (Z.Q.); cxu6@uwo.ca (C.X.); Tel.: +86-0791-88171689 (Z.Q.)

Abstract: Cold-rolling oily sludge contains high amounts of oil and iron resources that can be recycled by pyrolysis. We investigated the pyrolysis behavior and volatile products of oily sludge by thermogravimetric analysis (TG) coupled with Fourier transform infrared spectroscopy (FTIR) and a pyrolyzer (PY) coupled with gas chromatography/mass spectrometry (GC/MS). The pyrolysis process was divided into three stages: H_2O drying and CO_2 desorption at low temperatures (below 393 K); the volatilization of low-molecular-weight organics and the covalent bond cleavage of C=C, C-O, and C-H in the medium-molecular-weight organics at medium temperatures (393–844 K); and chain scission of the high-molecular-weight organics and reduction of iron oxides by CO at high temperatures (above 844 K). The weight losses of oily sludge in the three stages were 0.4 wt %, 47.9 wt %, and 14.7 wt %, respectively. According to the kinetic models, stage 2 and stage 3 could be described with the second-order and third-order reaction models, and their activation energies were 40.22 kJ/mol and 214.99 kJ/mol, respectively. The compounds in the volatile products were identified by FTIR and GC/MS. The organics in the volatile products from stage 2 pyrolysis mainly consisted of aliphatic hydrocarbons, fatty acids, esters, ketones, and nitrogen compounds, while the volatile products from stage 3 predominantly contained aliphatic hydrocarbons, mononuclear aromatic hydrocarbons, and small amounts of nitrogen compounds and CO, suggesting the occurrence of chain scission of heavy organics.

Keywords: cold-rolling oily sludge; pyrolysis; kinetic analysis; volatile composition

Citation: Que, Z.; Fu, Y.; Shi, J.; Ai, X.; Xu, C. Pyrolysis and Volatile Evolution Behaviors of Cold-Rolling Oily Sludge. *Processes* **2022**, *10*, 543. https://doi.org/10.3390/pr10030543

Academic Editors: Jun Han, Erhong Duan and Lin He

Received: 7 January 2022
Accepted: 9 March 2022
Published: 11 March 2022

1. Introduction

Cold-rolling oily sludge, produced from the cold rolling process, is an extremely complex three-phase mixture of lubricating oil, water, and iron fines [1–3]. Oily sludge treated with improper handling can seriously impact human health and lead to severe environmental pollution due to its toxicity [4–6]. In particular, since the high concentration of mineral oil in cold-rolling oily sludge has strong carcinogenic properties [7], it is included on the National Hazardous Waste List in China [8]. Moreover, due to the high contents of mineral oil and Fe in cold-rolling oily sludge, it can be a valuable resource for recovering high calorific oil and Fe [9,10].

To achieve resource recovery and alleviate hazards to the environment, several thermal-based treatments have been adopted, such as incineration, combustion, reduction, and pyrolysis. Incineration is a process of complete combustion of oily sludge in a controlled environment with excess air and auxiliary fuels [6,11], which is currently the mainstream method for disposing cold-rolling oily sludge. At a high temperature under an oxidizing atmosphere, the oil in the cold-rolling oily sludge is burned out, and Fe, FeO, and Fe_3O_4 are oxidized to Fe_2O_3. Although the cold-rolling oily sludge is completely mineralized in this method, the organic matters in the oil phase are not recovered. Meanwhile, the method has the disadvantage of high energy consumption and the production of secondary pollutants

such as SO_X, NO_X, dioxins, and heavy metals [12–15]. In addition, Volodymyr et al. [16] and Zhao et al. [17] studied the utilization of steel-rolling oily sludge in the iron ore sintering process and found that the sintering temperature, particle size, and tumbler index decreased when increasing the mass fraction of the rolling oily sludge from 0% to 3%. However, with a high proportion of the rolling oily sludge in the sintered mixture, incomplete combustion of liberated oil during the sintering process can create problems with gas cleaning and may even lead to damage of the equipment. Furthermore, in order to make full use of the oil-phase energy content and take advantage of the catalytic characteristic of iron oxides for pulverized coal combustion, Wang et al. [18] mixed the steel-rolling oily sludge with pulverized coal for blast furnace injection, aiming to realize the utilization of oily sludge resources and improve the combustion efficiency of pulverized coal, and found that the promotion efficiency was low when the proportion of the rolling oily sludge exceeded 10 wt %. Li et al. [19] attempted to dispose steel-rolling oily sludge by the coking process, at a low blending ratio of less than 0.5 wt %. Furthermore, Park et al. [20] and Martín et al. [21] recovered metallic iron from the hot-rolling oily sludge by the direct reduction method with coke dust and blast furnace slag. Compared with incineration, combustion, or reduction, pyrolysis treatment of steel-rolling oily sludge has received increasing attention recently, owing to its mild operation conditions, high treatment efficiency, high energy recovery, and generation of fewer pollutants [6,11,22,23]. Pyrolysis of oily sludge was studied in a fluidized bed reactor for the recovery of energy and iron by Qin et al. [24], Li et al. [25], and Lu et al. [26], who investigated pyrolysis of rolling oily sludge and obtained its kinetics at different temperatures. During the heat treatment of steel-rolling oily sludge, the organic matters in the oil phase were volatilized and cracked, and at the same time, volatile gases were generated. However, the thermal decomposition and volatile evolution behavior of steel-rolling oily sludge have not been simultaneously investigated. Hence, in this paper, the pyrolysis behavior and volatile products of a cold-rolling oily sludge were investigated by thermogravimetric analysis (TG) coupled with Fourier transform infrared spectroscopy (FTIR) and pyrolyzer (PY) coupled with gas chromatography/mass spectrometry (GC/MS). The kinetics and mechanisms of cold-rolling oily sludge pyrolysis were examined with the TGA data, and the volatile products generated were analyzed online by FTIR/GC-MS for their composition.

2. Materials and Methods

2.1. Materials

For this study, the raw oily sludge was collected from the cold rolling process of a steel plant in China. The cold-rolling oily sludge consists of moisture, oil, and solids. The moisture content of the raw cold-rolling oily sludge is 27.15 wt % (according to the Chinese standard GB/T 212–2008). To avoid the interference of water in the analysis, part of the raw oily sludge was dewatered under 50 °C for 120 h to obtain dried oil sludge. The proximate analysis of the dried cold-rolling oily sludge was carried out according to the Chinese standard GB/T 212–2008. Meanwhile, the carbon (C), hydrogen (H), nitrogen (N), and sulfur (S) analyses were performed on a CHNS analyzer (VarioEL III, Elementar, Germany). The mineral elements of the dried cold-rolling oily sludge were analyzed by ICP-MS (OPTIMA8000DV, PerkinElmer, USA). The dried cold-rolling oily sludge was characterized using scanning electron microscopy (Prisma E, Thermo Fisher Scientific, USA).

In order to clarify the composition of the oil phase and solid phase in the cold-rolling oily sludge, the solid and oil phases were separated by Soxhlet extraction in Dichloromethane solvent. The solid phase was analyzed using an X-ray fluorescence spectrometer (PANalytical Axios, PANalytical B.V., The Netherlands) and an X-ray diffractometer (D8 Advance, Bruker, Germany). The oil phase was diluted by chromatographically pure hexane, and the volume ratio of oil phase and chromatographically pure hexane was 1:50. The diluted sample was analyzed by a quadrupole GC/MS (5977B-7820A, Agilent, USA). The split ratio was 30:1, using 1.0 mL/min purity helium as the carrier gas, and GC was equipped with the chromatographic column of HP-5MS (25 m × 0.25 mm × 0.25 μm, Agilent). During the

GC/MS analysis, the programmed temperature started at 323 K and was held for 5 min, then increased to 523 K at a rate of 5 K/min. It was held at 523 K for 10 min, and then raised to 573 K with the heating rate of 20 K/min and kept isothermal for 3 min.

2.2. TG-FTIR Analysis

Thermogravimetric analysis was conducted with a thermogravimetric analyzer (STA 449F3, Netzsch, Germany) coupled with a Fourier transform infrared spectrometer (FTIR) (Frontier, PerkinElmer, USA). Before the analysis, about 10 mg of the dried cold-rolling oily sludge was loaded in a ceramic crucible. The sample was heated in 80 mL/min helium flow from room temperature to 1573 K at 10 K/min. In addition, the solid residue was analyzed by the CHNS analyzer (VarioEL III, Elementar, Germany), X-ray diffractometer (D8 Advance, Bruker, Germany), and X-ray fluorescence spectrometer (PANalytical Axios, PANalytical B.V., The Netherlands).

2.3. Kinetic Analysis Theory

In this work, the pyrolysis of the cold-rolling oily sludge was carried out under non-isothermal conditions in a heterogeneous reaction system, where the rate of pyrolysis reaction can be described by the following equation:

$$\frac{d\alpha}{dT} = \frac{1}{\beta}k(T)f(\alpha) \tag{1}$$

where α is the conversion degree, %; T is the reaction temperature, K; β is the heating rate, K/min; $k(T)$ is the reaction rate constant which can be expressed by the Arrhenius equation; and $f(\alpha)$ is the differential mechanism function.

In each run, α can be obtained as follows:

$$\alpha = \frac{m_0 - m_t}{m_0 - m_f} \tag{2}$$

where m_0, m_t, and m_f are the initial weight of the sample at each stage, the weight of the sample at a certain time of the pyrolysis process, and the final weight of the solid at the end of the pyrolysis process, respectively.

According to the Arrhenius equation:

$$k(T) = Ae^{-\frac{E_a}{RT}} \tag{3}$$

where A is the pre-exponential factor, min^{-1}; E_a is the activation energy, J/mol; and R is the universal gas constant, 8.314 J/(K·mol).

By replacing $k(T)$ with Equation (3), Equation (1) can be written as:

$$\frac{d\alpha}{f(\alpha)} = \frac{A}{\beta}\exp\left(-\frac{E_a}{RT}\right)dT \tag{4}$$

The integral form of Equation (4) can be written as:

$$G(\alpha) = \int_0^\alpha \frac{d\alpha}{f(\alpha)} = \int_{T_0}^T \frac{A}{\beta}\exp\left(-\frac{E_a}{RT}\right)dT \tag{5}$$

where $G(\alpha)$ is the integrated form of the mechanism function $f(\alpha)$ and T_0 is the initial temperature of the pyrolysis reaction.

Coats–Redfern (C-R) is a classical method of model fitting, which we employed in this work to analyze the pyrolysis kinetics of the cold-rolling oily sludge. Equation (5) can be converted to [27]:

$$G(\alpha) = \int_0^\alpha \frac{d\alpha}{f(\alpha)} = \int_{T_0}^T \frac{A}{\beta}\exp\left(-\frac{E_a}{RT}\right)dT = \frac{A}{\beta}\frac{RT^2}{E_a}\left(1 - \frac{2RT}{E_a}\right)\exp\left(-\frac{E_a}{RT}\right) \tag{6}$$

Taking the logarithmic transformation on Equation (6) leads to:

$$\ln\left[\frac{G(\alpha)}{T^2}\right] = \ln\left[\frac{AR}{\beta E_a}\left(1-\frac{2RT}{E_a}\right)\right] - \frac{E_a}{RT} \quad (7)$$

Since the value of E_a is much larger than that of $2RT$, $\left(1-\frac{2RT}{E_a}\right)$ can be approximated to 1.0. Hence, by linear fitting $\ln\left[\frac{G(\alpha)}{T^2}\right]$ versus $\frac{1}{T}$, the values of the activation energy E_a and the pre-exponential factor A can be calculated by the slope and the intercept of the straight line. The most frequently used kinetic mechanism functions for solid-state reactions are shown in Table 1 [28].

Table 1. The most widely used kinetic mechanism functions for solid-state reactions [28].

Mechanism Model	Symbol	*f(α)*	*G(α)*
Chemical reaction			
First-order	F_1	$1-\alpha$	$-\ln(1-\alpha)$
Second-order	F_2	$(1-\alpha)^2$	$(1-\alpha)^{-1}-1$
Third-order	F_3	$(1-\alpha)^3$	$\left[(1-\alpha)^{-1}-1\right]/2$
Diffusion			
One-way transport	D_1	0.5α	α^2
Two-way transport	D_2	$[-\ln(1-\alpha)]^{-1}$	$(1-\alpha)\ln(1-\alpha)+\alpha$
Three-way transport	D_3	$1.5(1-\alpha)^{2/3}\left[1-(1-\alpha)^{1/3}\right]^{-1}$	$\left[1-(1-\alpha)^{1/3}\right]^2$
Ginstling–Brounshtein equation	D_4	$1.5\left[(1-\alpha)^{1/3}-1\right]^{-1}$	$(1-2\alpha/3)-(1-\alpha)^{2/3}$
Random nucleation growth			
1.5-dimensional	$A_{1.5}$	$1.5(1-\alpha)[-\ln(1-\alpha)]^{1/2}$	$[-\ln(1-\alpha)]^{2/3}$
Two-dimensional	A_2	$2(1-\alpha)[-\ln(1-\alpha)]^{1/2}$	$[-\ln(1-\alpha)]^{1/2}$
Three-dimensional	A_3	$3(1-\alpha)[-\ln(1-\alpha)]^{1/2}$	$[-\ln(1-\alpha)]^{1/3}$
Limiting surface reaction			
One dimension	R_1	1	α
Two dimensions	R_2	$2(1-\alpha)^{1/2}$	$1-(1-\alpha)^{1/2}$
Three dimensions	R_3	$3(1-\alpha)^{1/3}$	$1-(1-\alpha)^{1/3}$

Reproduced with permission from Chunxiang Chen, Xiaoqian Ma, Yao He; Bioresource Technology; published by Elsevier, 2012.

2.4. Py-GC/MS Experiments

The pyrolyzer (Rx-3050TR, Frontier, Japan) coupled with a quadrupole GC/MS (7820A-5977B, Agilent, USA) were used to investigate product distributions during the pyrolysis process of cold-rolling oily sludge. The dried cold-rolling oily sludge in the pyrolyzer was heated in two stages at 10 K/min: the first stage was from 393 K to 844 K and the second stage was between 844 K and 1173 K. The volatiles within a selected temperature range, produced by 0.8 mg of the dried cold-rolling oily sludge, were trapped at the forepart of the column by liquid nitrogen. At the same time, the generated volatiles were carried by pure helium gas at 1.0 mL/min at a split ratio of 30:1 into the GC equipped with the chromatographic column of HP-5MS (25 m × 0.25 mm × 0.25 μm, Agilent). During the GC/MS analysis, the programmed temperature started at 313 K and was held for 1 min, then increased to 473 K at a rate of 4 K/min. It was held at 473 K for 5 min, and then was raised to 563 K with the heating rate of 3 K/min and kept isothermal for 10 min.

3. Results and Discussion

3.1. Characterization of Cold-Rolling Oily Sludge

Table 2 shows the proximate and ultimate analyses of the dried cold-rolling oily sludge. The moisture contents decreased from 27.152 wt % in the raw sludge to 1.63 wt % in the dried sludge. The volatile content of the dried sludge was 62.33 wt %. Due to the oxidation of Fe and Fe_3O_4 in the air, it was difficult to accurately measure the ash and fixed carbon contents. Their contents were lumped and calculated by difference in this work, amounting

to 36.04 wt %. The H/C element ratio of the dried cold-rolling oily sludge was about 0.1428, and the contents of N and S elements were 0.14 wt % and 0.49 wt %, respectively. Figure 1 shows the SEM images and EDS spectra of the dried sludge. The cold-rolling oily sludge contained fine metal particles with uniform distribution of Fe, C, O, Al, and S, of which Fe was the predominant element. The elements' contents of the solid phase in the dried cold-rolling oily sludge are listed in Table 3. As expected, Fe and O were found to be the main elements in the solid phase of the cold-rolling oily sludge. The X-ray diffraction pattern of the solid phase in dried cold-rolling oily sludge is illustrated in Figure 2, further evidencing that the solid phase of the cold-rolling oily sludge contained iron metal (Fe) and magnetite (Fe_3O_4). Figure 3 shows the GC-MS chromatograms of the oil phase, and the main organic compounds with a relative content of more than 0.10% (area %) in the oil phase are listed in Table 4 The oil phase was mainly composed of fatty acids such as n-hexadecanoic acid and cis-13-octadecenoic acid, and the mass fraction of them was about 82.772%, while the mass fractions of aliphatic hydrocarbons, esters, ketones, aldehydes, nitrogen compounds, and sulfur compounds were 0.507%, 1.790%, 0.741%, 0.241%, 7.643%, and 0.669%, respectively.

Table 2. Proximate and ultimate analyses of the dried cold-rolling sludge.

Proximate Analysis (wt %)			Ultimate Analysis (wt %)			
Moisture	**Volatile**	**Fixed Carbon + Ash** [1]	**C**	**H**	**N**	**S**
1.63	62.33	36.04	41.36	6.13	0.14	0.49

[1] By difference.

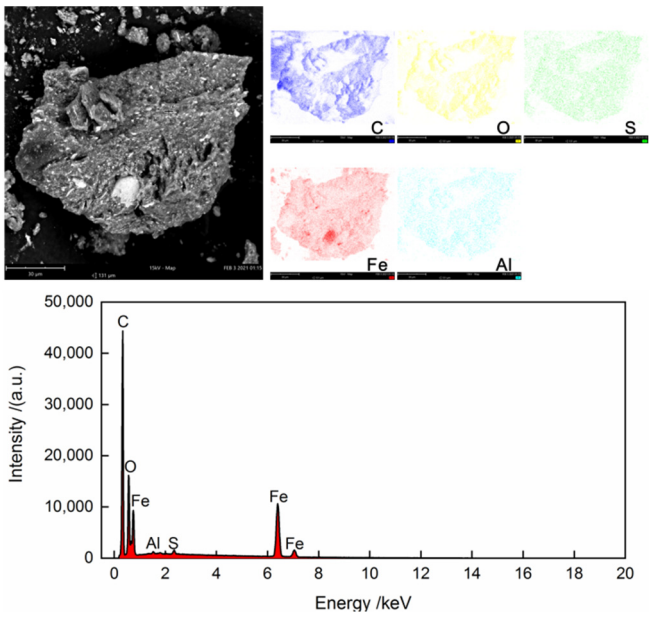

Figure 1. SEM images and EDS spectra of the dried cold-rolling oily sludge.

Table 3. Element analyses of the solid phase in the cold-rolling oily sludge by XRF (wt %).

Fe	O [1]	Cl	S	Cu	Ni	Cr	As	Si
66.089	29.673	2.684	0.507	0.154	0.148	0.131	0.120	0.110
Mn	Al	Ca	P	Zn	Mo	Br	Ge	
0.109	0.064	0.055	0.054	0.049	0.022	0.016	0.015	

[1] By difference.

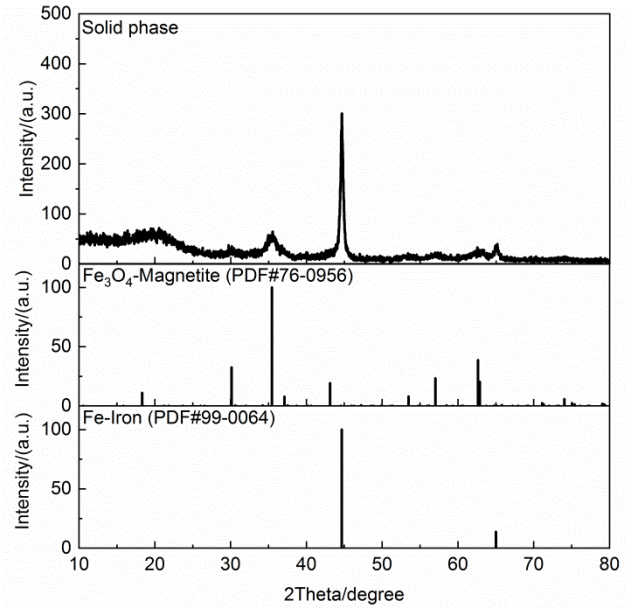

Figure 2. XRD pattern of the solid phase in the dried cold-rolling oily sludge.

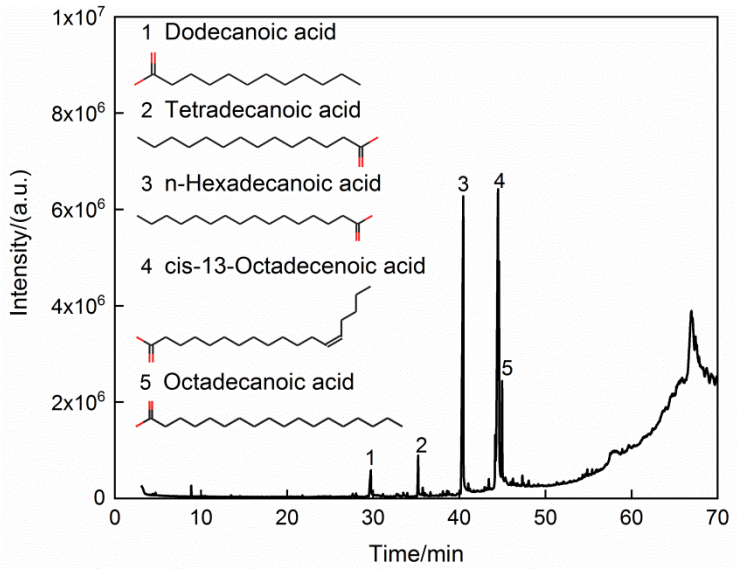

Figure 3. GC-MS chromatograms of the oil phase.

Table 4. Compents of the oil phase in the cold-rolling oil sludge by GC/MS.

Name of Compounds	RT /min	Formula	Area /%
Aliphatic hydrocarbons			
2,6-Octadiene, 2,4-dimethyl-	3.113	$C_{10}H_{18}$	0.137
Cetene	27.612	$C_{16}H_{32}$	0.158
Cyclohexane, ethenyl-	46.232	C_8H_{14}	0.212
Sub Total			**0.507**
Fatty acids			
Dodecanoic acid	29.717	$C_{12}H_{24}O_2$	2.591
Tetradecanoic acid	35.217	$C_{14}H_{28}O_2$	2.209
n-Hexadecanoic acid	40.457	$C_{16}H_{32}O_2$	33.364
cis-13-Octadecenoic acid	44.499	$C_{18}H_{34}O_2$	27.384
cis-13-Octadecenoic acid	44.605	$C_{18}H_{34}O_2$	12.433
Octadecanoic acid	44.966	$C_{18}H_{36}O_2$	4.791

Table 4. *Cont.*

Name of Compounds	RT /min	Formula	Area /%
Sub Total			**82.772**
Esters			
Adipic acid, ethyl 4-heptyl ester	29.726	$C_{15}H_{28}O_4$	0.406
cis-3-Nonen-1-ol, 2-methylpropionate	31.121	$C_{13}H_{24}O_2$	0.103
Phosphonofluoridic acid, ethyl-, decyl ester	35.747	$C_{12}H_{26}FO_2P$	0.135
Hexadecanoic acid, ethyl ester	41.036	$C_{18}H_{36}O_2$	0.214
4-[N′-(4-Methoxy-benzoyl)-hydrazino]-4-oxo-butyric acid methyl ester	44.506	$C_{13}H_{16}N_2O_5$	0.398
Phosphoric acid, tris(4-methylphenyl) ester	54.318	$C_{21}H_{21}O_4P$	0.103
Phosphoric acid, tris(4-methylphenyl) ester	54.869	$C_{21}H_{21}O_4P$	0.269
Phosphoric acid, tris(4-methylphenyl) ester	55.425	$C_{21}H_{21}O_4P$	0.162
Sub Total			**1.791**
Ketones			
Pentadecanal-	33.951	$C_{15}H_{30}O$	0.127
Pentadecanal-	36.640	$C_{15}H_{30}O$	0.126
2(3H)-Furanone, 5-dodecyldihydro-	43.415	$C_{16}H_{30}O_2$	0.378
2-Heptyne-4-one	45.367	$C_7H_{10}O$	0.110
Sub Total			**0.742**
Aldehydes			
(Z)-Undec-6-en-2-one	38.089	$C_{11}H_{20}O$	0.102
10-Undecenal	38.572	$C_{11}H_{20}O$	0.139
Sub Total			**0.241**
Nitrogen compounds			
1-Ethanone, 2-[(2-hydroxyphenyl)imino]-1,2-diphenyl-	40.444	$C_{20}H_{15}NO_2$	0.391
Phenol, 4-bromo-2-nitro-	44.174	$C_6H_4BrNO_3$	0.884
2-Amino-4-hydroxy-6-methylpyrimidine	44.485	$C_5H_7N_3O$	5.716
Pyrazolo[1,5-a]pyrimidine, 2-methyl-7-phenyl-	44.616	$C_{13}H_{11}N_3$	0.139
1-(Prop-2-ynyl)-3,3-pentamethylenediaziridine	47.316	$C_9H_{14}N_2$	0.344
Urea, 1-[2-(2-methyl-1H-indol-3-yl)ethyl]-3-propyl-	48.064	$C_{15}H_{21}N_3O$	0.169
Sub Total			**8.021**
Sulfur compounds			
2-Heptanethiol, 2-methyl-	8.865	$C_8H_{18}S$	0.415
Disulfide, bis(1,1,3,3-tetramethylbutyl)	35.743	$C_{16}H_{34}S_2$	0.254
Sub Total			**0.669**
Unresolved Area			**5.236**
Total			**100.00**

3.2. Pyrolysis Behavior of Cold-Rolling Oily Sludge

Figure 4 shows the thermogravimetry (TG) and differential thermogravimetry (DTG) curves of the dried cold-rolling oily sludge at the heating rate of 10 K/min in a helium atmosphere. As shown in Figure 4, there were three stages during the decomposition process of the sludge between 293 K and 1573 K. Figure 5 shows the FTIR spectra of the evolved volatile gas products from pyrolysis at 393 K, 597 K, and 1071 K. Table 5 illustrates the infrared absorption peaks of major gaseous products [28,29]. In the initial stage at the temperature below 393 K, TG and DTG curves declined slightly, with about 0.4 wt % weight loss. The FTIR spectra of gas products at 393 K (Figure 5a) display obvious absorption bands at 4000–3500 cm^{-1} and 2000–1250 cm^{-1}, attributed to the O–H bonds of the water. The absorption bands at 2400–2250 cm^{-1} and 667 cm^{-1} can be attributed to CO_2. This suggests that H_2O and CO_2 were released from the cold-rolling oily sludge in stage 1 pyrolysis, likely due to the drying and gas desorption [30]. During the second stage, in the temperature range from 393 K to 844 K, the TG curve dropped rapidly, resulting in the largest weight loss peak shown by the DTG curve (3.02 wt %·min^{-1}) at 597 K. The total weight loss of stage 2 pyrolysis was approximately 47.9 wt %. The FTIR spectra of volatile gas products at 597 K (Figure 5b) show an absorption band of C-H bonds at 3000–2800 cm^{-1}, implying the release of alkyl groups along with the absorption bands of

H_2O and CO_2. At the same time, the C=O bond at around 1780–1640 cm^{-1} reveals the possible presence of esters, carboxylic acids, and ketones [29]. The low-molecular-weight components in the cold-rolling oily sludge could thermally decompose and volatilize. In the last stage (stage 3), at temperatures above 844 K, the weight loss during was 14.7 wt %, with a weight loss rate of 1.83 wt %·min^{-1} at 1071 K. As seen from Figure 5c, the IR peaks of CO at 2181 and 2109 cm^{-1} and C-H bonds at 3000–2800 cm^{-1} were observed in the volatile gas from the sludge at 1071 K, suggesting that heavy carbonaceous substances in the residues of the cold-rolling oily sludge cracked to form CO and alkyl groups at a high temperature. In addition, the IR peaks of CO_2 at 2400–2250 cm^{-1} and 667 cm^{-1} indicate that the iron oxide in the solid phase could be reduced by the CO to form CO_2 [26].

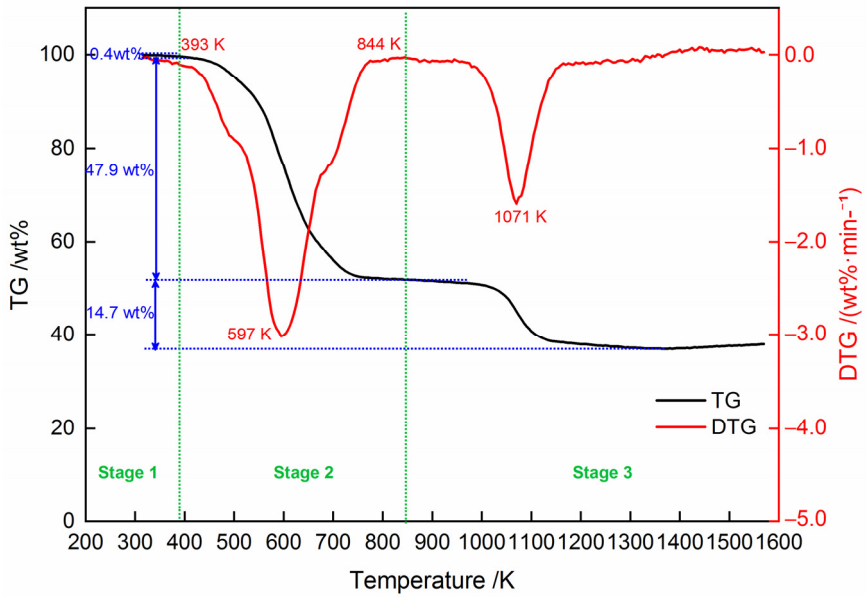

Figure 4. TG and DTG curves of the dried cold-rolling oily sludge heated in helium at the heating rate of 10 K/min.

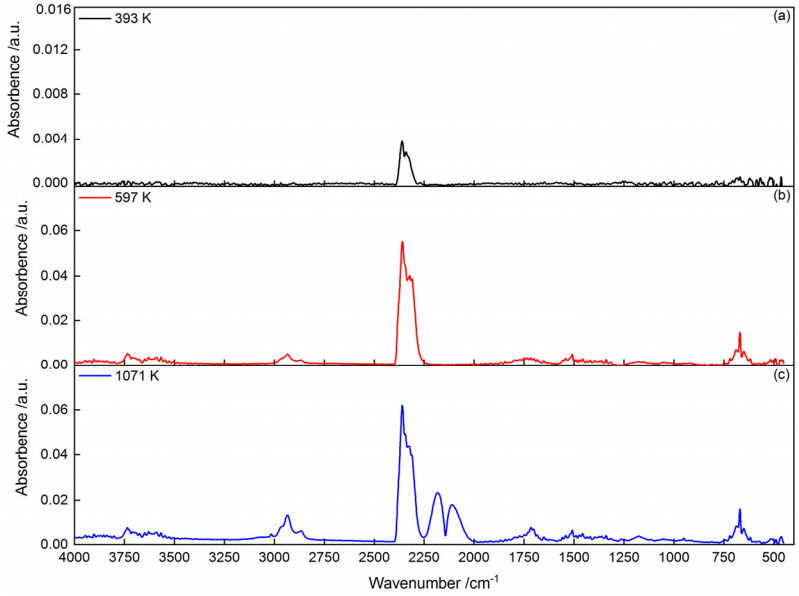

Figure 5. FTIR spectra of volatile gas products from the cold-rolling oily sludge pyrolysis at different temperatures: (**a**) 393 K; (**b**) 597 K; (**c**) 1071 K.

Table 5. IR absorption bands for the volatile gas products from cold-rolling oil sludge pyrolysis and the corresponding vibration types of the species.

Species	Absorption (cm^{-1})	Functional Groups	Vibrations
H_2O	4000–3400 cm^{-1}	O-H	Stretching
	2000–1200 cm^{-1}	O-H	In-plane bending
CO_2	2400–2230 cm^{-1}	C=O	Stretching
	667 cm^{-1}	C=O	Out-plane bending
CO	2181 and 2116 cm^{-1}	C≡O	Stretching
Alkyl groups	3000–2800 cm^{-1}	C-H	Stretching
Carboxylic acids	3000–2800 cm^{-1}	C-H	Stretching
	1780–1640 cm^{-1}	C=O	Stretching
Esters	1440–1375 cm^{-1}	O-H	In-plane bending
	950–890 cm^{-1}	O-H	Out-plane bending
	3000–2800 cm^{-1}	C-H	Stretching
	1780–1640 cm^{-1}	C=O	Stretching

3.3. Kinetic Analysis

In order to clarify the kinetics of the cold-rolling oily sludge pyrolysis, the pyrolysis process was modeled by the Coats–Redfern method for stage 2 and stage 3. During the heating process of cold-rolling oily sludge, devolatilization of low-molecular-weight organics, decomposition of heavy organics, and reduction of CO and residues occurred, which can be usually described by chemical reaction, diffusion, random nucleation growth, and limiting surface reaction mechanisms [29]. The values of E_a and A calculated by 15 kinds of related mechanism models are shown in Table 6. Based on the correlation coefficient (R^2), the closer to 1 the better, and the most probable mechanism functions for stage 2 and stage 3 are the second-order and third-order reaction models, respectively, with the E_a values determined to be 40.22 kJ/mol and 214.99 kJ/mol, respectively. The activation energy of stage 2 is obviously lower than that of stage 3. During the pyrolysis process of the cold-rolling oily sludge, when the temperature was below 844 K, the low boiling point volatiles (low-molecular-weight organic compounds) were almost all devolatilized, and the covalent bonds of the medium-molecular-weight organic compounds were broken, leading to the largest weight loss (48.3 wt %), accounting for 76.7% of the total weight loss in the entire pyrolysis process. The devolatilization process at stage 3 had the largest activation energy, likely due to thermal decomposition of the heavy carbonaceous substances and the reduction reaction between the CO and iron oxides, leading to 14.7 wt % weight loss.

Table 6. E_a, A, and R^2 in various mechanism models calculated by the Coats–Redfern method.

Model Symbol	Stage 2			Stage 3		
	E_a (kJ/mol)	A (min^{-1})	R^2	E_a (kJ/mol)	A (min^{-1})	R^2
F_1	40.22	2.10×10^2	0.9786	138.61	2.71×10^5	0.8749
F_2	66.35	2.57×10^5	0.9593	214.99	6.59×10^9	0.9498
F_3	99.51	1.47×10^9	0.8795	311.82	1.97×10^{15}	0.9253
D_1	64.14	6.24×10^3	0.8863	218.72	3.33×10^8	0.7689
D_2	69.69	1.43×10^4	0.9159	235.34	1.56×10^9	0.7996
D_3	78.68	3.52×10^4	0.9560	261.87	1.16×10^{10}	0.8448
D_4	72.49	6.73×10^3	0.9301	243.63	1.04×10^9	0.8146
$A_{1.5}$	23.62	5.86×10^0	0.9686	86.44	6.97×10^{-1}	0.8579
A_2	15.32	7.93×10	0.9530	60.36	3.13×10	0.8376
A_3	7.02	7.57×10^2	0.8829	34.27	1.14×10^0	0.7843
R_1	27.28	5.82×10^0	0.8392	100.41	1.45×10^3	0.7353
R_2	32.31	1.25×10	0.9132	115.37	5.78×10^3	0.7985
R_3	34.55	1.58×10	0.9379	121.98	9.53×10^3	0.8232

3.4. Compositions of the Solid Residue Generated during Oily Sludge Pyrolysis

Table 7 shows the ultimate analyses of the solid residue. There were no H and N elements, and the contents of C and S elements were 2.51 wt % and 1.53 wt %, respectively. The H/C element ratio decreased from 0.1428 in the dried cold-rolling oily sludge to 0 in the solid residue. This indicates that there were no organic matters in the solid residue. The X-ray diffraction pattern of the solid residue is illustrated in Figure 6. It shows that the solid residue also contained iron metal (Fe) and magnetite (Fe_3O_4). The solid residue was analyzed by XRF, and the results are shown in Table 8. The mass fraction of the element Fe increased from 66.089% in the solid phase of the dried cold-rolling oily sludge to 96.075% in the solid residue, due to the reduction of Fe_3O_4 to Fe by organic matters during the pyrolysis process. The solid residue had a high content of iron metal, no organic matter, and little inorganic carbon and other metal elements, which could be directly used as the raw material for iron ore sintering and EAF steelmaking. Moreover, the iron metal and biochar can be separated from the solid residue by magnetism, and the iron metal can be used to produce strong magnetic materials such as NdFeB.

Table 7. Ultimate analyses of the solid residue (wt %).

C	H	N	S
2.51	0.00	0.00	1.53

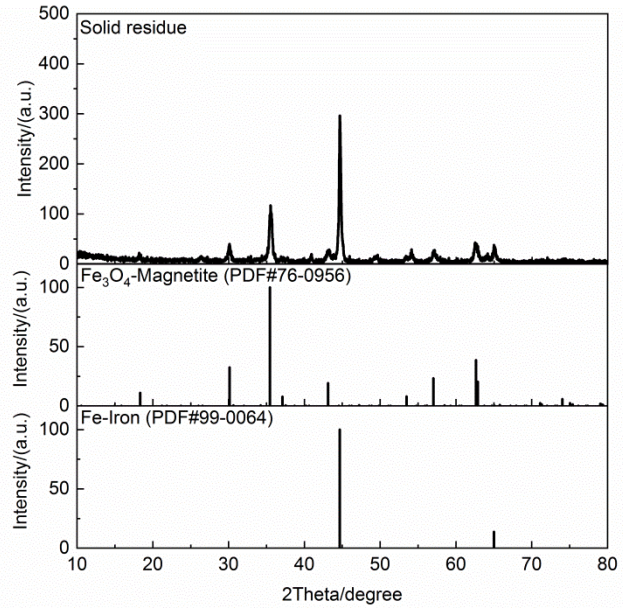

Figure 6. XRD patterns of the solid residue generated during oily sludge pyrolysis.

Table 8. Ultimate analyses of the solid residue (wt %).

Fe	S	Si	Al	As	Cu	Ni	Co	Cr
96.075	1.551	0.603	0.43	0.263	0.221	0.156	0.155	0.149
Mn	P	Mo	K	Ti	Ge	Ca	Cl	
0.136	0.108	0.037	0.033	0.028	0.023	0.018	0.014	

3.5. Compositions of Volatile Products Generated during Oily Sludge Pyrolysis

Figure 7 shows GC/MS chromatograms of volatile products from oil sludge pyrolysis at 393–844 K and 844–1173 K. Comparing the MS spectrum with the NIST database, the main organic compounds with a relative content of more than 0.1% (area %) in the volatile products are listed in Table S1 and their classification in Table 9. Figure 5a shows that the aliphatic

hydrocarbons had the high intensity, followed by fatty acids, such as n-hexadecanoic acid and dodecanoic acid. According to Table 7, the organics in the volatile products mainly consist of aliphatic hydrocarbons (C_3–C_{15}), fatty acids such as n-hexadecanoic acid and dodecanoic acid, ketones, esters, and nitrogen compounds at 393–844 K, at relative contents of 37.133%, 11.684%, 11.327%, 7.346%, and 9.028%, respectively. These compounds could be mainly formed by cleavage of C=C, C-O, and C-H bonds in most fatty acids and by volatilization of the low-molecular-weight components of aliphatic hydrocarbons and nitrogen compounds in the cold-rolling oily sludge. Furthermore, at 844–1173 K, there were fewer species of organic compounds detectable by GC-MS, mainly propene, benzene, toluene, and a small amount of nitrogen compounds, and the relative contents of aliphatic hydrocarbons, monocyclic aromatic hydrocarbons, and nitrogen compounds were 49.780%, 36.594%, and 5.431%, respectively. At high temperatures, the C=O bonds in the high-molecular-weight components of esters and fatty acids were broken to form aliphatic hydrocarbons and CO. At the same time, the Fe_3O_4 in the solid phase was reduced to Fe by CO. In addition, nitrogenous benzenes were pyrolyzed to form monocyclic aromatic hydrocarbons and nitrogen compounds. Yu et al. [31] found that Fe can promote the cleavage of phenol and nitrogen-containing compounds, so the cleavage of nitrogenous benzenes was promoted by Fe in the solid phase. In view of the volatile products, since the aliphatic hydrocarbons and monocyclic aromatic hydrocarbons are usually gaseous at room temperature and do not contain PAHs, they can be used as basic raw materials for petrochemicals and fuels. The fatty acids and esters could act as surfactants.

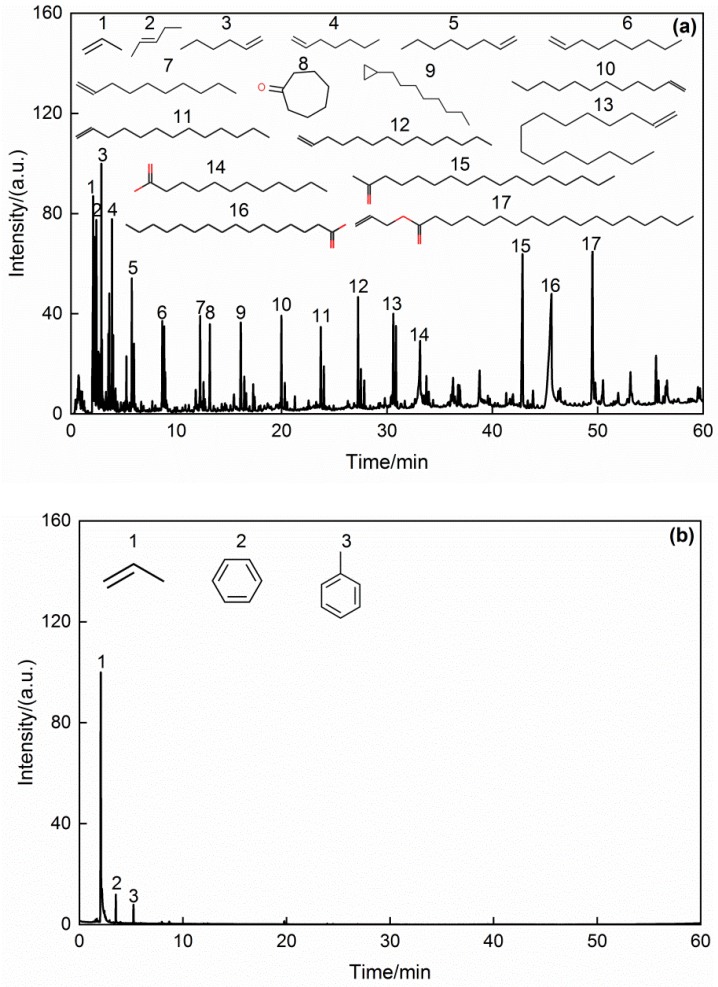

Figure 7. GC/MS chromatograms of volatile products from cold-rolling oil sludge pyrolysis at different temperatures: (**a**) 393–844 K; (**b**) 844–1173 K.

Table 9. Classification of volatile products from cold-rolling oil sludge pyrolysis by GC/MS (area %).

Compounds	Aliphatic Hydrocarbons	Monocyclic Aromatic Hydrocarbons	Fatty Acids	Esters	Ketones	Aldehydes	Nitrogen Compounds	Others
Volatile products at 393–844 K	37.133	2.912	11.684	7.346	11.327	1.050	9.028	19.520
Volatile products at 844–1173 K	49.780	34.627	0.000	0.000	1.211	2.123	5.431	4.861

4. Conclusions

(1) The pyrolysis process of cold-rolling oily sludge can be divided into three stages and the weight loss was 0.4 wt % at low temperatures (below 393 K), 47.9 wt % at medium temperatures (393–844 K), and 14.7 wt % at high temperatures (844–1173 K).

(2) H_2O was evaporated and CO_2 was desorbed in the first stage; the low-molecular-weight components of aliphatic hydrocarbons and nitrogen compounds were volatilized and the C=C, C-O, and C-H bonds in the fatty acids broken in the second stage; and the heavy organics cracked to form aliphatic hydrocarbons, monocyclic aromatic hydrocarbons, and CO, and iron oxides were reduced by CO in the third stage. Stages 2 and 3 of the pyrolysis process could be described by the second-order and third-order reaction models, with the activation energies of 40.22 kJ/mol and 214.99 kJ/mol, respectively.

(3) The volatile products mainly consist of aliphatic hydrocarbons (C_3–C_{15}), fatty acids, esters, ketones, and nitrogen compounds in the second stage, and predominantly aliphatic hydrocarbons, monocyclic aromatic hydrocarbons, and small amounts of nitrogen compounds and CO in the third stage. The volatile products could be used as basic raw materials for petrochemicals and fuels. The solid residue could be directly returned to iron ore sintering and EAF steelmaking, or iron metal could be separated as a raw material for the production of magnetic materials.

Supplementary Materials: The following supporting information can be downloaded at: https://www.mdpi.com/article/10.3390/pr10030543/s1, Table S1: compents of the volatile products from cold-rolling oil sludge pyrolysis by GC/MS at 393–844 K and 844–1173 K.

Author Contributions: Conceptualization, C.X. and Z.Q.; methodology, Y.F.; software, Y.F.; validation, X.A. and J.S.; formal analysis, J.S.; investigation, Z.Q.; resources, X.A.; data curation, Y.F.; writing—original draft preparation, Z.Q.; writing—review and editing, C.X.; visualization, Z.Q.; supervision, J.S.; project administration, J.S.; funding acquisition, Z.Q. All authors have read and agreed to the published version of the manuscript.

Funding: This research was funded by the National Natural Science Foundation of China (no. 51904127 and no. 51166004), the Key R&D Program of Jiangxi Province (no. 20202BBGL73117 and no. 20201BBE51013), and the Pilot Demonstration Project for the Contract Responsibility System of the Provincial Science and Technology Plan Project of Jiangxi Academy of Sciences (no. 2021YSBG21015).

Institutional Review Board Statement: Not applicable.

Informed Consent Statement: Not applicable.

Data Availability Statement: All data are available and can be shared upon request.

Conflicts of Interest: The authors declare no conflict of interest.

References

1. Biswal, B.K.; Tiwari, S.N.; Mukherji, S. Biodegradation of oil in oily sludges from steel mills. *Bioresour. Technol.* **2009**, *100*, 1700–1703. [CrossRef] [PubMed]
2. Fu, Y.; Que, Z.; Ai, X.; Zou, W.; Deng, T.; Shi, J. Study on three-phase ratio and composition of rolling-steel oily sludge. *Energy Res. Manag.* **2021**, *8*, 97–101. [CrossRef]
3. Iluţiu-Varvara, D.-A.; Aciu, C.; Pică, E.M.; Sava, C. Research on the chemical characterization of the oily mill scale for natural resources conservation. *Procedia Eng.* **2017**, *181*, 439–443. [CrossRef]

4. Fuentes, S.; Barra, B.; Caporaso, J.G.; Seeger, M. From rare to dominant: A fine-tuned soil bacterial bloom during petroleum hydrocarbon bioremediation. *Appl. Environ. Microbiol.* **2016**, *82*, 888–896. [CrossRef] [PubMed]
5. Taheri, A.; Taheri, A.; Fathivand, A.A.; Mansouri, N. Risk assessment of naturally occurring radioactive materials (NORM) in the hydrocarbon sludge extracted from the south pars gas field in Iran. *Process Saf. Environ. Prot.* **2019**, *125*, 102–120. [CrossRef]
6. Teng, Q.; Zhang, D.; Yang, C. A review of the application of different treatment processes for oily sludge. *Environ. Sci. Pollut. Res.* **2021**, *28*, 121–132. [CrossRef]
7. Obi, L.; Atagana, H.; Adeleke, R.; Maila, M.; Bamuza-Pemu, E. Potential microbial drivers of biodegradation of polycyclic aromatic hydrocarbons in crude oil sludge using a composting technique. *J. Chem. Technol. Biotechnol.* **2020**, *95*, 1569–1579. [CrossRef]
8. Luo, X.; Gong, H.; He, Z.; Zhang, P.; He, L. Research on mechanism and characteristics of oil recovery from oily sludge in ultrasonic fields. *J. Hazard. Mater.* **2020**, *399*, 123137. [CrossRef]
9. Liu, B.; Zhang, S.; Tian, J.; Pan, D.; Liu, Y.; Volinsky, A.A. Recycle of valuable products from oily cold rolling mill sludge. *Int. J. Miner. Metall. Mater.* **2013**, *20*, 941–946. [CrossRef]
10. Liu, B.; Zhang, S.; Tian, J.; Pan, D.; Meng, L.; Liu, Y. New technology for recyclingmaterials from oily cold rollingmill sludge. *Int. J. Miner. Metall. Mater.* **2013**, *20*, 1141–1147. [CrossRef]
11. Hu, G.; Feng, H.; He, P.; Li, J.; Hewage, K.; Sadiq, R. Comparative life-cycle assessment of traditional and emerging oily sludge treatment approaches. *J. Clean. Prod.* **2020**, *251*, 119594. [CrossRef]
12. Gong, Z.; Liu, L.; Zhang, H.; Wang, Z.; Wu, J.; Guo, Y.; Zhang, J. Study on the migration characteristics of As, Pb, and Ni during oily sludge incineration with CaO additive. *Energy Fuels* **2020**, *34*, 16341–16349. [CrossRef]
13. Wang, Z.; Liu, L.; Gong, Z.; Zhang, H.; Wu, J. Study on the ecological risk of heavy metals during oily sludge incineration with CaO additive. *J. Environ. Sci. Health Part A* **2021**, *56*, 797–803. [CrossRef] [PubMed]
14. Li, C.T.; Lee, W.J.; Mi, H.H.; Su, C.C. PAH emission from the incineration of waste oily sludge and PE plastic mixtures. *Sci. Total Environ.* **1995**, *170*, 171–183. [CrossRef]
15. Zhao, R.; Qin, J.; Chen, T.; Wang, L.; Wu, J. Experimental study on co-combustion of low rank coal semicoke and oil sludge by TG-FTIR. *Waste Manag.* **2020**, *116*, 91–99. [CrossRef]
16. Shatokha, V.I.; Gogenko, O.O.; Kripak, S.M. Utilising of the oiled rolling mills scale in iron ore sintering process. *Resour. Conserv. Recycl.* **2011**, *55*, 435–440. [CrossRef]
17. Zhao, H.; Zhong, W.; Zhou, G.; Shao, Y.; Wang, T.; Liu, F.; Jin, B.S. Experimental research on utilization of steel rolling sludge in sintering process. *Int. J. Chem. Reactor Eng.* **2013**, *11*, 283–291. [CrossRef]
18. Wang, Y.; Zou, C.; Li, J.; Liu, Z.; Zhao, J.; Wang, W. Combustion performance of blast furnace pulverizedcoal mixed with metallurgical sludge. *Iron Steel* **2021**, *55*, 115–122. [CrossRef]
19. Jian, L.; Xiaoming, M.; Desheng, H. Foundational research on the treatment of oily sludge by coking process. *Baosteel Technol.* **2018**, *2*, 39–45. [CrossRef]
20. Parka, J.W.; Ahna, J.C.; Songa, H.; Parka, K.; Shina, H.; Shu, A.J. Reduction characteristics of oily hot rolling mill sludge by direct reduced iron method. *Resour. Conserv. Recycl.* **2002**, *34*, 129–140. [CrossRef]
21. Martín, M.I.; López, F.A.; Torralba, J.M. Production of sponge iron powder by reduction of rolling mill scale. *Ironmak. Steelmak.* **2013**, *39*, 155–162. [CrossRef]
22. Song, Q.; Zhao, H.; Jia, J.; Zhang, F.; Wang, Z.; Lv, W.; Yang, L.; Zhang, W.; Zhang, Y.; Shu, X. Characterization of the products obtained by pyrolysis of oil sludge with steel slag in a continuous pyrolysis-magnetic separation reactor. *Fuel* **2019**, *255*, 115711. [CrossRef]
23. Wang, Z.; Gong, Z.; Wang, Z.; Li, X.; Chu, Z. Application and development of pyrolysis technology in petroleum oily sludge treatment. *Environ. Eng. Res.* **2020**, *26*, 190460. [CrossRef]
24. Qin, L.; Han, J.; He, X.; Zhan, Y.; Yu, F. Recovery of energy and iron from oily sludge pyrolysis in a fluidized bed reactor. *J. Environ. Manag.* **2015**, *154*, 177–182. [CrossRef] [PubMed]
25. Liang, Q.; Han, D.; Cao, Z.; Du, J. Studies on kinetic and reaction mechanism of oil rolling sludge under a wide temperature range. *Energy Sources Part A* **2021**. [CrossRef]
26. Lu, W.; He, P.; Shao, L.; Zhang, H. Pyrolysis of rolling oil sludge and its kinetic analysis. *China Environ. Sci.* **2017**, *37*, 1024–1030. [CrossRef]
27. Nie, F.; Li, Y.; Tong, K.; Wu, B.; Zhang, M.; Ren, W.; Xie, S.; Li, X. Volatile evolution during thermal treatment of oily sludge from a petroleum refinery wastewater treatment Plant: TGA-MS, Py-GC(EGA)/MS and kinetics study. *Fuel* **2020**, *278*, 118332. [CrossRef]
28. Chen, C.; Ma, X.; He, Y. Co-pyrolysis characteristics of microalgae Chlorella vulgaris and coal through TGA. *Bioresour. Technol.* **2012**, *117*, 264–273. [CrossRef]
29. Chen, J.; Mu, L.; Jiang, B.; Yin, H.; Song, X.; Li, A. TG/DSC-FTIR and Py-GC investigation on pyrolysis characteristics of petrochemical wastewater sludge. *Bioresour. Technol.* **2015**, *192*, 1–10. [CrossRef]
30. Song, W.; Liu, J.; Nie, Y. Pyrolysis behaviors of oil sludge based on TG/FTIR and PY-GC/MS. *Front. Environ. Sci. Eng. China* **2010**, *4*, 59–64. [CrossRef]
31. Yu, G.; Chen, D.; Arena, U.; Huang, Z.; Dai, X. Reforming sewage sludge pyrolysis volatile with Fe-embedded char: Minimization of liquid product yield. *Waste Manag.* **2018**, *73*, 464–475. [CrossRef] [PubMed]